Aberystwyth University

Characterization, localization and temporal expression of crustacean hyperglycemic hormone (CHH) in the behaviorally rhythmic peracarid crustaceans, Eurydice pulchra (Leach) and Talitrus saltator (Montagu)

Hoelters, Laura Sophie; O'Grady, Joseph Francis; Webster, Simon George; Wilcockson, D.

Accepted Manuscript

Characterization, localization and temporal expression of crustacean hyperglycemic hormone (CHH) in behaviorally rhythmic peracarid crustaceans, *Eurydice pulchra* (Leach) and *Talitrus saltator* (Montagu)

Laura Hoelters, Joseph Francis O'Grady, Simon George Webster, David Charles Wilcockson

Please cite this article as: Hoelters, L., O'Grady, J.F., Webster, S.G., Wilcockson, D.C., Characterization, localization and temporal expression of crustacean hyperglycemic hormone (CHH) in behaviorally rhythmic peracarid crustaceans, *Eurydice pulchra* (Leach) and *Talitrus saltator* (Montagu), *General and Comparative Endocrinology* (2016), doi: http://dx.doi.org/10.1016/j.ygcen.2016.07.024

Characterization, localization and temporal expression of crustacean hyperglycemic hormone (CHH) in behaviorally rhythmic peracarid crustaceans, *Eurydice pulchra* (Leach) and *Talitrus saltator* (Montagu)

Laura Hoelters[a], Joseph Francis O'Grady[a], Simon George Webster[b] and David Charles Wilcockson*[a,b].

a. Institute of Biological, Environmental and Rural Sciences, Aberystwyth University, Penglais, Aberystwyth, Ceredigion, SY23 3DA, UK

b. School of Biological Sciences, Bangor University, Brambell Building, Deiniol Road, Bangor, Gwynedd, LL57 2UW, UK.

*Email of corresponding author: dqw@aber.ac.uk

Email addresses of authors:

Laura Hoelters: lsh8@aber.ac.uk; Joseph O'Grady: joefogrady@gmail.com; Simon Webster: s.g.webster@bangor.ac.uk; David Wilcockson: dqw@aber.ac.uk

Abstract

Crustacean hyperglycemic hormone (CHH) has been extensively studied in decapod crustaceans where it is known to exert pleiotropic effects, including regulation of blood glucose levels. Hyperglycemia in decapods seems to be temporally gated to coincide with periods of activity, under circadian clock control. Here, we used gene cloning, *in situ* hybridization and immunohistochemistry to describe the characterization and localization of CHH in two peracarid crustaceans, *Eurydice pulchra* and *Talitrus saltator.* We also exploited the robust behavioral rhythmicity of these species to test the hypothesis that CHH mRNA expression would resonate with their circatidal (12.4 h) and circadian (24 h) behavioral phenotypes. We show that both species express a single *CHH* transcript in the cerebral ganglia, encoding peptides featuring all expected, conserved characteristics of other CHHs. *E. pulchra* preproCHH is an amidated 73 amino acid peptide N-terminally flanked by a short, 18 amino acid precursor related peptide (CPRP) whilst the *T. saltator* prohormone is also amidated but 72 amino acids in length and an associated 56 residue CPRP. The localization of both was mapped by immunohistochemistry to the protocerebrum with axon tracts leading to the sinus gland and into the tritocerebrum, with striking similarities to terrestrial isopod species. We substantiated the cellular position of CHH immunoreactive cells by *in-situ* hybridization. Although both species showed robust activity rhythms, neither exhibited rhythmic transcriptional activity indicating that CHH transcription is not likely to be under clock control. These data make a contribution to the inventory of CHHs that is currently lacking for non-decapod species.

Keywords

1. Introduction

In crustaceans increased metabolic demands levied by periods of activity are met by hyperglycemia and available evidence points to the central role of crustacean hyperglycemic hormone (CHH) in regulating blood sugar levels. Whilst carbohydrate metabolism was the first identified function of CHH, it is now firmly established that it is a pleiotropic hormone involved in many other physiological processes including regulation of ion and salt balance, gamete maturation, ecdysis (reviews: Webster, 2015; Webster et al., 2012).

An important site of CHH synthesis in malacostracans is the X-organ, located in the medulla terminalis of the optic ganglia (MTXO). In decapod crustaceans the cells of the XO project axons distally along the ventro-lateral margin of the eyestalk where they coalesce to form a neurohemal organ, the sinus gland. Serotonergic inputs to the MTXO are believed to invoke the release of CHH into the ophthalmic artery for circulation (Escamilla-Chimal et al., 2002; Santos et al., 2001). CHHs have been described from several neural tissues: pericardial organs (Chung and Zmora, 2008; Dircksen et al., 2001; Keller et al., 1985), cerebral ganglia (Nelson-Mora et al., 2013), ventral nerve cord (Chang et al., 1999), retinal tapetal cells (Escamilla-Chimal et al., 2001) and in non-neural tissues including the fore and hind-gut (Webster et al., 2000).

The ability of an organism to anticipate and respond to regular changes in the environment is imperative to its fitness. Accordingly, prokaryotes and eukaryotes have evolved time-keeping mechanisms that enable them to synchronize their behavior and physiology to predictable cyclic events. In the terrestrial realm organisms cope with diurnal changes in the environment by having a daily timekeeper- the so-called circadian clock that has a period of about 24 hours. In contrast, in the marine intertidal the principle environmental cues affecting organisms are associated with lunar events and include circatidal cycles of immersion and emersion (12.4 hours) and circasemilunar (c.15 day) cycles of tidal amplitude modulation.

For several decades it has been known that in decapod crustaceans, blood glucose levels follow a diurnal pattern in temporal correspondence with daily

activity cycles (Gorgels-Kallen and Voorter, 1985; Kallen et al., 1990; Tilden et al., 2001). This cyclic hyperglycemia mirrors (with a phase delay of about 2 h) elevated CHH titers in the hemolymph (Kallen et al., 1990) and available evidence suggests that this results from episodic synthesis, transport and release of CHH from the sinus gland (Gorgels-Kallen and Voorter, 1985; Kallen et al., 1990). An immunohistochemical study in the nocturnal crayfish *Astacus leptodactylus* revealed that CHH synthesis, axon transport to the sinus gland and subsequent exocytosis were timed to ensure release of CHH, and consequent hyperglycemia, occurred about 2 hours prior to expected night-time during the animal's activity phase (Gorgels-Kallen and Voorter, 1985). Similar outcomes were reported in a study on *Orconectes limosus*; CHH hemolymph titers and glucose levels peaked coincident with nocturnal activity (Kallen et al., 1990). The endogenous, light entrainable nature of this circadian rhythm of hyperglycemia has been demonstrated experimentally in *A. leptodactylus* (Kallen et al., 1988).

More recently, Nelson-Mora et al. (2013) investigated the expression dynamics of *CHH* mRNA in the crayfish *Procambarus clarkii* over a day/night cycle in both entrained LD and free-running (DD) conditions. Their data provide evidence for a circadian rhythm of *CHH* transcription. Intriguingly they also found *CHH* transcripts and (crucially) anti-CHH immunoreactivity in the central brain in several proto- and tritocerebral cell clusters known to express canonical clock proteins such as Timeless, Period and Clock (Bmal) (Escamilla-Chimal et al., 2010). These observations, taken together with the finding reported by the same authors that CHH immunoreactivity was recorded in both cytoplasm and nuclei of the brain CHH cells (akin to circadian clock transcriptional repressor nuclear translocation events), led to the interpretation that a relationship exists between the central circadian clock and CHH.

It is not yet clear whether periods of heightened activity are generally associated with hyperglycemia, or are governed by outputs from circadian or circatidal oscillators. An attractive approach would be to characterise and measure CHH transcripts, as well as describing the localisation of these and their cognate peptides in rhythmic animals using two model systems- one driven a by tidal

(12.4 h) chronometric mechanism and the other by circadian clock. To this end we examined the expression of CHH mRNAs in two species of peracarid crustaceans, the isopod, *Eurydice pulchra* and amphipod *Talitrus saltator* that both display robust rhythmic behavioral phenotypes. *E. pulchra* inhabits the mean high water mark of sandy shores of North Western Europe where it remains buried at low tide, emerging to swim, feed and breed when the tide returns. Accordingly it shows robust, endogenous circatidal (~12.4 h) activity cycles entrained to tidal inundation (Alheit and Naylor, 1976; Hastings, 1981a; Zhang et al., 2013) and circatidal metabolic rhythms (Hastings, 1981b; O'Neill et al., 2015). In addition, circadian modulation of circatidal activity and daily pigment (chromatophore) migration are under the control of a separate circadian system (Zhang et al., 2013). In contrast *T. saltator* exhibits only diurnal behavior, resting buried in sand in the supra-littoral during daytime, emerging after nightfall to forage. This activity is governed by an endogenous circadian system (Bregazzi and Naylor, 1972). We reasoned that, given their robust and tractable behavioral phenotypes with both 24 h and tidal periods, these two species represent excellent candidates for measuring the expression of the CHH transcript(s). Thus, we hypothesized that in *E. pulchra* and *T. saltator*, *CHH* mRNA would cycle with 24 h and 12.4 h periods respectively. Here, we describe the characterization and sequence of a single type-I CHH cDNA in the cerebral ganglia of each species, the cellular localization of CHH and its mRNA and the transcriptional dynamics of the CHH gene over daily and tidal cycles in behaviorally rhythmic individuals.

2. Materials and methods

2.1 Identification and full length sequencing of CHH cDNA in *Talitrus saltator* and *Eurydice pulchra*

RNA extraction and cDNA
Animals were decapitated and heads immediately frozen in liquid nitrogen. For cDNA cloning, total RNA was extracted from head tissues from both species. Total RNA was extracted with Trizol® and *DNAse* treated with 2 U Turbo™ *DNAse*

(Ambion, UK). RNA was subsequently quantified on a Nanodrop ND2000 spectrophotometer (LabTech, UK) and 500 ng reverse transcribed with SuperScript® III reverse transcriptase (Life Technologies, UK). Complementary DNA for 5' and 3' rapid amplification of cDNA ends (RACE) PCR was made from 1 µg total RNA using the GeneRacer™ cDNA kit (Life Technologies, UK) and SuperScript® III according to the manufacturers instructions. For qPCR, 500 ng total RNA was reverse transcribed using High Capacity Reverse Transcription reagents in 20 µl volumes and using the supplied random hexamer primers (Life Technologies, UK).

2.2 *Eurydice pulchra* CHH cDNA sequencing

A semi-nested PCR strategy was used to amplify the 3' end of the *Eurydice pulchra* CHH cDNA using a fully degenerate forward primer (Echh Degen 3' RACE, See Supplementary Table 1 for full list of primers used) designed against the conserved amino acid sequence (VCEDCYN, positions 22-28 in *Carcinus maenas* CHH) with touchdown PCR cycling conditions. All reagents were supplied by Life Technologies, UK unless otherwise stated. Reactions were done with Platinum® Taq PCR mix and included 1 µl of the F' primer at 100 µM and 1 µl of GeneRacer 3' RACE primer in a 20 µl final volume. Cycling conditions were, 94°C 3 min activation followed by 1 cycle of 94°C 30 sec, 68°C 2 min, 5 cycles of 94°C 30 sec, 68°C 1 min, 5 cycles of 94°C 30 sec, 64°C 1 min, and 25 cycles of 94°C 30 sec, 50°C 1.5 min, with a final extension at 68°C for 15min. This initial PCR was followed by a second round of amplification using 1 µl of first round PCR product as template. Reactions were done in 20 µl volumes using Megamix Blue polymerase mastermix (Helena Biosciences, Gateshead, UK) and the same Echh Degen 3' RACE degenerate primer but with 1 µl of the GeneRacer 3' N reverse primer. Cycling conditions were 95°C 5 mins activation followed by 35 cycles of 95°C 45 sec, 50°C 60 sec and 72°C 60 sec, and a final extension for 7 min at 72°C. Amplicons were resolved on 2% agarose gels and strong positive bands excised, extracted (QIAquick® Gel Clean-up kit, Qiagen, UK) and cloned into TOPO pCR™4-TOPO® and transformed (One Shot® TOP10') according to manufacturer's guidelines. Plasmid DNA was extracted (QIAprep, Qiagen) from

positive colonies containing the correct size insert as determined by *EcoR1* digestion (5U for 1 hour at 37°C) and sequenced in-house.

To amplify the 5' end of the *E. pulchra* CHH cDNA sequence information from the 3' RACE was used to design gene specific primers for 5' RACE. Initial PCR reactions were done with Platinum® Taq PCR mix in 20 µl reaction volumes containing 1 µl of 5' RACE primer (10 µM) and the GeneRacer 5' primer. Cycling conditions were 94°C for 3 mins activation followed by 35 cycles of 94°C 30 secs, 55°C 45 secs and 72°C 1 min and a final extension of 72°C for 7 mins. A second, nested PCR amplification was done using 1 µl of the initial PCR reaction as template and containing 5' RACE and GeneRacer 5' N primers (1 µl each). Cycling conditions were identical as for the first round PCR but with Megamix Blue PCR mastermix (Helena Biosciences). Products were resolved on a 2% agarose gel and cloned and sequenced as described above.

2.3 *Talitrus saltator* CHH cDNA sequencing

A putative CHH cDNA sequence was mined from a *Talitrus saltator* brain transcriptome generated by Illumina RNAseq sequencing and annotated with Blast2GO software (O' Grady, 2013). To obtain full-length sequence and to confirm the assembled contig sequence, a RACE PCR and cloning strategy was used. Briefly, conventional RT-PCR was done with 1 µl Talchh F' and Talchh R' primers (10 µM) with Amplitaq Gold® 360 mastermix in a 20 µl reaction volume using brain cDNA as template. Cycling conditions were 94°C 5 mins activation followed by 35 cycles of 94°C 30s, 55°C 45s and 72°C 1 min and a final extension for 7 mins at 72°C. Products were resolved on a 2% agarose gel and bands of the expected size were excised, cloned and sequenced as described above. For 3' RACE, 3 rounds of nested PCR were done. The first PCR was done with Amplitaq Gold® 360 mastermix and 1 µl of each Talchh 3' RACE and GeneRacer 3' primers and 1 µl 3' RACE cDNA with identical cycling conditions as for *T. saltator* CHH RT-PCR. A second round amplification was done in an identical fashion but with Talchh 3' N1 GeneRacer 3' N primers with 1 µl of the first PCR as template. Finally, a third PCR was done in the same way with Talchh 2' N2 and the

GeneRacer 3'N primer and 1 µl of the second round PCR as template with the same cycling conditions except that only 30 cycles were run. Products were resolved on a 2% agarose gel and amplicons of the expected size excised and sequenced as described above.

2.4 Quantitative Reverse transcription PCR (qRT-PCR)

Quantitative RT-PCR was done using Applied Biosystems TaqMan® MGB hydrolysis probes 5' labelled with FAM as described previously (Sharp et al., 2010). Sequences and positions for TaqMan primers and probes are given in Supplementary Table 1. RNA was extracted and reverse transcribed as detailed above. Standard curves in the range 1×10^{11} copies per µl for qPCR were made from cRNA produced by *in vitro* transcription using DNA templates amplified from brain cDNA and using T7 phage promoter-flanked PCR primers (Supplementary Table 1). Quantitative RT-PCR (qRT-PCR) was done using Applied Biosystems Universal Taqman® PCR mix or Bioline Sensimix™ Probe mastermix containing the internal reference dye, ROX, according the manufacturers recommendations. Each 20 µl reaction contained 0.5 µl each primer (10 µM) and probe (2.5 µM) and 1 µl cDNA. qPCR reactions for *E. pulchra* CHH were run in singleplex and data normalised to the reference transcript *Erpl32* (Accession number, CO157254). *TalCHH* was measured in duplex reactions with the internal reference gene *TalAK* mined from the above mentioned brain transcriptome (O' Grady, 2013). We investigated several candidate reference genes and found that for *E. pulchra*, only *Erpl32* provided reliable normalization over time-course sampling and assay (Zhang et al., 2013). For *T. saltator*, we also tested multiple candidates including β-actin and α-tubulin but only *arginine kinase* proved sufficiently reliable. Quantitative PCRs were run in duplicate or triplicate on either an Applied Biosystems 9700 or QuantStudio™ 12K Flex machine with the following cycling conditions: 50°C 2min, 95°C 10 mins and then 40 cycles of 95°C 15s and 60°C, 60s (Taqman® PCR mix); 95°C 10 mins followed by 40 cycles of 95°C 15s and 60°C, 60s (Bioline Sensimix Probe™). For each assay, standards in serial ten-fold dilutions were run in the range 10^9-10^3 copies per reaction. PCR efficiencies were in the range 90-100%. Data were expressed as copies *CHH* per copy of the internal reference transcript.

2.5 Behavioral analysis

E. pulchra were caught using hand trawled 1mm-mesh nets from Llandonna
Beach, Anglesey, UK. Activity recordings of were done using *Drosophila* activity
monitors (DAM10, Trikinetics, MA) exactly as previously reported (Zhang et al
2013) on animals taken directly form the shore.   Activity of *E. pulchra* was
recorded in constant darkness (DD) over three tidal cycles to check for
rhythmicity before heads were harvested into liquid nitrogen at 3 h intervals (10
pooled heads per replicate) for qPCR. *T. saltator* were collected from Ynyslas
beach, Wales, UK and held in damp sand under 12:12LD for seven days prior to
analysis. Since *T. saltator* has been shown to express more robust and less
variable locomotor rhythms in small groups, (Bregazzi and Naylor, 1972)
animals were housed in groups of five in a glass tank containing 10 cm-deep
damp sand and compartmentalized with Plexiglas dividers. Thus, each chamber
of five individuals was treated as a single replicate. Across each compartment
infra red beams were passed via bespoke recording apparatus (fabricated by
Trikinetics, MA) on the same principles as the DAM10 monitors. Activity for both
species, registered as interruptions to infrared beams, was recorded via
proprietary software and analyzed and plotted using ClockLab (Actimetrics, IL)
run via Matlab® v6.2.

2.6 *In-situ* hybridization

In-situ hybridization was done using digoxygenin-labelled riboprobes as
previously described (Wilcockson et al., 2011). Probe synthesis was performed
using primers detailed in Supplementary Table 1. Preparations were mounted in
50% glycerol/PBS and imaged under a light microscope and prepared (cropped,
resized and adjusted for brightness and contrast) with Adobe Photoshop CS6.

2.7 Immunocytochemistry

Cerebral ganglia were dissected from animals held in DD and during the
expected photophase, under ice-chilled physiological saline and immediately
fixed in Stefanini's fixative (Stefanini et al., 1967) for 12 h at 4°C. Following
fixation brains were washed extensively in 0.1 M PB (pH 7.5) containing 0.25%

Triton X-100 (PTX). Brains were then incubated in primary antibody (anti-*Carcinus maenas* CHH IgG, 25 µg/µl, raised in rabbit and fully characterized by Chung and Wesbter (2004)) at 1:5000 in PTX overnight at 4°C. Subsequently tissues were washed in PTX 3x 10 minutes, 3x 30 minutes. Secondary antisera (Alexa 488 for *E. pulchra* and Alexa 568 for *T. saltator*, Molecular Probes, UK) were applied in PTX at 1:500 and incubated overnight at 4°C followed by washing in PTX as described above. Tissues were mounted in Vectashield® (Vectorlabs, UK) and visualized using a Leica TCS SP5 II confocal microscope. Confocal images were based on a Z-stack of 15–25 optical sections taken at 1–2 µm intervals and were prepared (cropped, resized and adjusted for brightness and contrast) using Adobe Photoshop CS6.

2.8 Phylogenetic analysis

Sequences for mature CHH peptides from a range of crustaceans were obtained via NCBI protein databases (for accession numbers see supplementary Figure S1 legend) and aligned in BioEdit v7.2.5 (Hall, 1999). Maximum likelihood trees were generated using MEGA 6 software (Tamura et al., 2013). All positions containing gaps and missing data were eliminated. Partial/pairwise deletion and Poisson corrected distances were performed, with 1000 bootstrap replications.

2.9 Statistical analysis

Gene expression data were analysed by one-way analysis of variance using Statistica software v8 (StatSoft, Tulsa, US).

3. Results

3.1 Characterization of cDNA encoding *Eurydice pulchra* and *Talitrus saltator* CHH

For *E. pulchra* CHH cDNA sequencing we used a degenerate PCR approach with primers directed at the conserved amino acid sequence (VCEDCYN, positions 22-28) followed by RACE PCR to elucidate the UTRs. This strategy yielded a single 616bp product the sequence of which is shown in Figure 1A (NCBI GenBank accession number JF927891). The sequence contains a 363 bp open reading

frame (ORF) encoding a preprohormone comprising a 27 amino acid signal peptide, a 76 amino acid CHH peptide C-terminally flanked by an 18 amino acid CHH precursor related peptide ending in a dibasic cleavage site (KR). The mature CHH contains an amidation signal (GKK).

For *T. saltator* we obtained a putative CHH cDNA sequence from an un-annotated Illumina sequenced transcriptome (O' Grady, 2013). From this we were able to perform conventional RT-PCR and 3', 5'RACE. This approach yielded an 1132bp sequence shown in Figure 1B (NCBI GenBank accession number KP898735). This sequence contains a 404 bp ORF encoding a preprohormone comprising a 24 amino acid signal peptide, a 75 amino acid CHH which is also C-terminally flanked by a 56 amino acid CPRP ending in a dibasic cleavage site (KR). The mature CHH terminates in an amidation signal (GKK).

3.2 Phylogenetic analysis

Both peracarid species grouped with the only other isopod sequence available, *A. vulgare,* and formed a discrete clade from all analyzed decapod species (Supplementary Figure S1). Included also in this clade were the water flea, *Daphnia magna* and the orthopteran, *Locusta migratoria*, both of which have ion transport peptide-like peptides (Webster et al., 2012). Amongst the decapods, clades formed groupings in accordance to their taxonomic positions.

3.3 Localization of *Eurydice pulchra* CHH peptide and mRNA in the cerebral ganglia

Immunofluorescent whole-mounted brains labelled using the IgG fraction of an anti-*Carcinus maenas* CHH serum resulted in clear and highly specific labelling that showed striking similarity to neuroarchitecture described in the woodlouse, *Oniscus asellus* (Nussbaum and Dircksen, 1995). Terminology used here refers to that of Nussbaum and Dircksen (1995).

Four anti-CHH IgG immunoreactive perikarya (27 µm +/-4 µm) in each brain hemisphere were localized in an anterior medial position, close to the midline and extending into the cleft between the two lobes of the anterior protocerebrum (PRC) (Figure 2A). Collaterals branching from a prominent axon tract and proximal to the cell bodies, form dendritic fields in the anterior PRC

close to the midline. From the primary tract, formed by the fasciculation of fibers from the cell group, axons extend dorsally before bifurcating, with one branch heading laterally into the optic lobe and the other descending into the tritocerebrum, adjacent to the orifice of the esophagus where they appear to terminate. The lateral branch travels along the posterior margin of the optic lobe terminating in an intensely labelled sinus gland (Figure 2B). The sinus gland is rather diffuse but with prominent axonal swellings and terminals. Wholemount *in situ* hybridization confirmed the localization of mRNAs encoding *E. pulchra* CHH was limited to four cells in each hemisphere of the anterior median PRC (Figure 2F).

3.4 Localization of *Talitrus saltator* CHH peptide and mRNA in the cerebral ganglia

The anti-CHH labelled neuroarchitecture revealed by wholemount immunofluorescence in *T. saltator* brains differed from that of the isopod in that two distinct cell groups were seen in the anterior margin of the PRC in each hemisphere (Figures 2D and 2E); a 'large' cell type (35 µm +/-4 µm) with 3 perikarya in each hemisphere and a 'small' cell type (23 µm +/-4 µm), also with 3 perikarya in each hemisphere. Both cell types had a granular cytoplasm and each appeared to project axons that contributed to the main tract. Close to the perikarya, collaterals formed dendritic fields, primarily posterior to the cell bodies adjacent to the midline. As seen in *E. pulchra*, the principal axon tract in *T. saltator* bifurcates with one branch turning laterally, before travelling along the posterior edge of the optic lobe to the sinus gland, and the other descending to into the tritocerebrum where they appeared to terminate adjacent to the margins of the esophageal orifice; here, labelling was observed in what appeared to be endings or dendritic fields (Figure 2D). Although difficult to determine their exact origin, these tritocerebral fibers presumably emerged as collaterals from the axon tract in the deuterocerebrum. The sinus glands were intensely labelled and, as seen in *E. pulchra,* were rather diffuse but with very clear axonal swellings and terminals (Figure 2C). Further evidence for two distinct cells types was provided by wholemount *in situ* hybridization in *T. saltator* brains when the large and small cell groups were clearly defined (Figure 2G).

3.5 Circadian and circatidal behavioral analysis

Both species, taken from their home beach and held in constant conditions, divorced from any environmental cues showed strongly rhythmic activity. *E. pulchra* showed robust and self-sustaining swimming activity with peak beam breaks coincident with expected high tides (Figure 3A and 3E). Periodogram analysis of these animals showed a mean period of 12.3 h (+/-0.04 h, sem, n=24) (Figure 3C). In addition, animals exhibited daily modulation of this tidal activity with maximal swimming shown on expected nighttime high tides (Figure 3E). *T. saltator* showed rhythmic locomotor activity at time of expected night (Figure 3B and 3F). Periodogram analysis revealed this rhythm to have a period of 24.18 h (+/- 0.3 h, sem, n=7) (Figure 3D).

3.6 CHH mRNA expression in rhythmic animals

We chose to measure the expression of *CHH* transcripts in *E. pulchra* and *T. saltator* using highly specific and sensitive Taqman® MGB hydrolysis probes. In animals showing strong and self-sustained activity rhythms, neither species showed any evidence of cyclic expression of *CHH* in head tissues harvested over a 24 h period (Figure 4). One-way ANOVA: *E. pulchra*, $F_{(7,24)}$ =1.19, P=0.35; *T saltator*, $F_{(8,53)}$=0.72, P=0.67.

4. Discussion

Despite being one of the largest orders in the Malacostraca, the Peracarida are poorly represented in terms of work on their neuroendocrine regulation. One complete CHH peptide has been characterized in the isopod *Armadillidium vulgare* by Edman degradation and mass spectrometry (Martin et al., 1993) and a partial sequence and amino acid composition of a CHH peptide has been elucidated from *Porcellio dilatatus* (Martin et al., 1984b). The former, a 73 residue peptide has an unblocked N-terminus and an amidated C-terminus and shares conserved CHH features with decapod peptides (Martin et al., 1993). In the present study we describe the deduced sequence of a type-I CHH in each of

the peracarid crustaceans *E. pulchra* and *T. saltator*. The CHH we describe for *E. pulchra* is 73 amino acids in length, in agreement with the CHH in *A. vulgar*e, whereas, in *T. saltator* the deduced mature CHH is 72 amino acids, in common with most decapods. Both contain cysteine residues at position 7-43, 23-39, 26-52, an invariant feature of type-1 CHHs and known to allow formation of 3 disulfide bridges. Sequence identity between the isopod CHHs in *A. vulgare* and *E. pulchra* is 79% (15/73) whilst that between *E. pulchra* and the amphipod *T. saltator* is 64% (26/72). Interestingly, *E. pulchra* CHH, in contrast to the both *A. vulgare* and *T. saltator,* is N-terminally blocked by pyroglutamate. Other species expressing unblocked CHHs include prawns (Chen et al., 2004; Davey et al., 2000; Gu et al., 2000; Lago-Leston et al., 2007; see also legend for supplementary Figure S1), the shrimp *Rimicaris kairei* (Qian et al., 2009) and the palinurid lobster *Jasus lalandii* (Marco et al., 1998). The only reported functional analysis of an isopod CHH was done in *A. vulgare* and showed that, in this species, CHH demonstrated no detectable molt or vitellogenesis inhibitory activity. Indeed, *A. vulgare* is known to express a separate VIH peptide (Azzouna et al., 2003; Greve et al., 1999).

The mature CHH peptides in both *E. pulchra* and *T. saltator* were C-terminally flanked by a putative CPRP of 18 and 56 amino acids respectively. The considerable difference in the sequence identity of these peptides is consistent with other species; the low level of conservation is a notable feature of CPRPs and, although these peptides are released into the hemolymph of crabs in stoichiometric relation to CHH, they have no defined function to date (Wilcockson et al., 2002).

Phylogenic analysis illustrated by the Maximum Likelihood tree places both species as a distinct clade grouped separately from the decapod relatives analyzed. This was not unexpected of course but, notably, the amphipod *T. saltator* occupies a position outside of the isopod clade that is grouped together with *Daphnia* (and an insect ion transport peptide). However, the relative paucity of sequence information for non-decapod species blunts resolution of these analyses and presumably contributes to this scenario.

In the isopods *A. vulgare*, *P. dilatatus*, *O. asellus* , *P. scaber* and *Ligia oceanicus* the median PRC is known to contain neurohormonal cells projecting axons into the sinus gland (Azzouna et al., 2003; Martin et al., 1984a; Nussbaum and Dircksen, 1995) . These are classed according to their histological and ultrastructural traits as β (β1 and β2), B, and γ cells (Martin 1988). Initially, antisera raised against crude sinus gland extracts were used (Martin et al., 1984a) to reveal immunoreactivity exclusively in β1 cells and axons of *P. dilatatus*. Subsequently, application of a more specific anti-CHH sera revealed staining in β1 (and also perhaps another two β2 cell groups) in *O. asellus* (Nussbaum and Dircksen, 1995) and strikingly similar structural organization of CHH staining in *A. vulgare* (Azzouna et al., 2003). In the current study the neuroarchitecture in both *E. pulchra* and *T. saltator* matched closely that described in detail for *O. asellus*. In *E. pulchra* we observed four cells per anterior median protocerebral hemisphere but we did not observe heterogeneity in gross morphological or labelling properties between the CHH producing cells. In *A. vulgare* the PRC contains only three CHH cells per hemisphere with the cell type conforming to the morphological description of β-cells (Azzouna et al., 2003). The number and position of CHH immunoreactive perikarya in *E. pulchra* was corroborated by whole-mount *in situ* hybridization and whilst we acknowledge this doesn't provide unequivocal evidence that these cells are synthesizing exclusively CHH, it does suggest that our immunolabelling is not a cross-reaction with other CHH-like hormones, such as VIH. In concord with the description of anti-CHH labelling in *O. asellus* (Nussbaum and Dircksen, 1995) we also observed intense staining in the sinus gland, more so than in the principle axonal trunk extending to the sinus glands from the eight perikarya in this species.

In contrast to the situation in the isopods, in *T. saltator* we observed two distinct cell types, one large (~35 μm) and one small (~23 μm) with three of each type per hemisphere. The classification of these cells is not clear; under our preparation protocols the smaller cells group appeared 'tear-drop' in shape and could feasibly correspond to the β2 subgroup described by Martin (1988). On the other hand, the nucleus of these cells appeared somewhat ovoid which is a diagnostic feature of subgroup β1 cells. Of course, the possibility remains that

these irregularities with the classification by Martin may be due to differences in our wholemount preparation protocol.

Intriguingly, scrutiny of the *T. saltator* CHH peptide sequence reveals the presence of a phenylalanine residue at position 3. In lobsters and crayfish, CHH undergoes post-translational L- to D- aminoacyl isomerization, primarily at residue 3 and is therefore present in L and D-Phe3 forms (Soyez et al., 1998; Soyez et al., 2000; Soyez et al., 1994; Yasuda et al., 1994). Using isoform specific antisera, it has been shown that these occupy different and distinct cells types in the medulla terminalis X-organ (Ollivaux et al., 2009). Therefore, it is tempting to speculate that, *T. saltator* CHH also undergoes this post-translational modification from the L- to D- enantiomer and the two CHH immunoreactive cell types correspond to those differentially synthesizing epimers of CHH. Such a scenario could have physiological implications; for example, the D-Phe3 CHH in palanurid lobsters confers prolonged bioactivity *in vivo* as a result of its recalcitrance to aminopeptidase degradation (Soyez, 2003). In Astacoidea, whilst the L-form of CHH is exclusively hyperglycemic, the D-Phe3 epimer exhibits moult-inhibitory (Yasuda et al 1994) and osmoregulatory activity (Serrano et al., 2003). Recently application of L- and D-Phe3 CHH isoforms and profiling of the hepatopancreas transcriptome indicates that the D-Phe3 form initiates short term but wide-ranging transcriptional regulation in this tissue, mainly down-regulation, compared to L-isoform (Manfrin et al., 2013). Regarding the current study, only application of antisera able to discriminate between these epimers in *T. saltator* will shed light on whether the cell types observed in the present study, in fact, contain modified peptides.

In both species we visualized fibers emanating form the primary axon tract and projecting caudally to terminate near to the margins of the esophageal orifice where they form a complex network of fine arborizations. We currently have no explanation for these features.

We set out to test the hypothesis that *CHH* mRNA expression resonates with behavioral rhythms in circadian and circatidal crustaceans. This objective was

based principally on a) the findings of Nelson-Mora et al (2013), who reported involvement of circadian time-keeping mechanisms and CHH mRNA expression and release in *Procambarus clarkii* and earlier work on crayfish suggesting circadian patterns of synthesis (Gorgels-Kallen and Voorter, 1985) and release of CHH (Gorgels-Kallen and Voorter, 1985; Kallen et al., 1990) and, b) that *E. pulchra* shows cyclic metabolic demands on a circatidal basis (Hastings, 1981b; O'Neill et al., 2015). We adopted a qRT-PCR approach, using highly sensitive and specific hydrolysis probes to measure brain CHH mRNA levels in *E. pulchra* and *T. saltator* that exhibited extremely robust and self-sustaining rhythms of locomotor activity, with c.12.4 h and 24 h and periods, respectively. Our expectation was that CHH expression would cycle with periodicities reflecting the behavioural rhythms in each species. In contrast to these expectations and to the reports of Nelson-Mora et al (2013), our analysis did not reveal significant changes in CHH mRNA levels over a 24 h period in either model. For *E. pulchra* at least, we know that the canonical clock gene *timeless* (*Eptim*), shows clear circadian cycling in the same RNA samples and using the same internal reference gene *Eprpl32* (Zhang et al., 2013), thus we are confident that our *CHH* data are a true reflection of the transcriptional activity in these samples. Even so, we can't discount the possibility that the pooled tissue samples (heads) necessary for this work may mask subtle rhythmicity in individual animal *CHH* expression. Indeed, close examination of the plotted data hint at bimodal expression of the mRNA with 'peaks' at 10 am and 10 pm, which correspond to 3 h prior to maximal swimming activity of the sampled animals. Whilst any changes in expression were extremely low (<2-fold), it is possible that, increased sampling intervals could yield evidence for tidal gene expression of *CHH*. *T. saltator* CHH mRNA showed little change in expression over the time-course samples. A caveat here is that endogenous rhythmicity of CHH synthesis might not be reflected in concomitant release patterns. Indeed, in the locust, there is an absence of coupling between release and biosynthesis (mRNA, peptide synthesis) of adipokinetic hormones- AKHs both *in vivo* (flight) and *in vitro* (peptides or signal transduction activators) (Harthoorn et al., 2001). Thus, we suggest that rather than clock-controlled, rhythmic synthesis of CHH, periodic release of stored CHH in the sinus glands could occur to satisfy the metabolic demands of *E.*

pulchra and *T. saltator*. Unfortunately, given the small size of the experimental organisms, measurement of circulating CHH even using our most sensitive immunoassays capable of measuring attomole quantites of CHH, is not feasible. Nevertheless, it would be worthwhile to investigate the ultrastructure of the sinus glands of each animal over a time-course to determine whether CHH is released in a rhythmic fashion as has been shown in crayfish (Gorgels-Kallen and Voorter, 1985). If temporal release was clock-controlled we predict that, in order to meet the metabolic demands of activity bouts, *E. pulchra* would show 12.4 h release cycles of CHH in contrast to 24 h circadian crustaceans. Given the apparent interaction of the CHH system with the circadian (and presumably circatidal) clock in these animals, studies testing this hypothesis might prove illuminating from a chronobiological perspective.

Descriptions of neurogenetic basis of oscillatory systems in crustaceans are limited. However (and, perhaps unsurprisingly) considerable homologies between insects and crustaceans circadian systems are emerging as more putative clock genes are sequenced in the latter (Tilden et al., 2011; Zhang et al., 2013). In an attempt to localize elements of the circadian clock in crayfish Escamilla-Chimal et al (2010) used a series of heterologous sera, raised against *Drosophila* TIM, PER and CLK to reveal immunoreactivity in the retina, optic ganglia and PRC (cell cluster 6). Cryptochrome immunoreactivity has also been demonstrated in the PRC (Escamilla-Chimal et al., 2010; Fanjul-Moles et al., 2004). In an elegant study by Beckwith et al. (2011), PDH-I from the crab *Cancer productus* was shown to co-localize with anti-CYC immunoreactive cells also in cell cluster 6 of the PRC. Moreover, expression of this PDH isoform, rescued rhythmicity in *pdf*-null mutant flies implicating PDH-1 as a PDF-like neuromodulator and molecular clock output. More recently, Nelson-Mora et al. (2013) demonstrated CHH immunoreactivity in the PRC cell cluster 6 of *P. clarkii,* and reported cytoplasmic and nuclear staining for CHH in these cells, reminiscent of the nuclear translocation of negative repressor molecules in *Drosophila* central oscillator cells. These findings were interpreted as CHH cells representing part of the circadian pacemaker system. Further evidence for connectivity between the CHH and circadian systems comes from findings that

CHH immunoreactive dendrites in the optic ganglia of crayfish receive serotonergic inputs and 5HT known to evoke CHH release (see review by Webster (2012) and references therein). Moreover, 5HT administered *in vivo* to lobster and crayfish modulates circadian rhythms, including phase shifts in the control of CHH release (Castanon-Cervantes et al., 1999). Thus, the emerging picture does indicate a link between the CHH and canonical circadian clock system but, to date, there is no definitive evidence for direct coupling of the two. We have previously described paired cells in each hemisphere that express the circadian clock protein Period in *E. pulchra* and localized these to the region of the brain corresponding to the dorso-lateral cells (in the "anterior medial cell cluster" (Sandeman et al., 1992)) (Zhang et al., 2013). These PER expressing cells do not match anatomically with the CHH cells described in this paper and we have no *prima face* evidence that they synapse with CHH perikarya, e.g. via protocerebral collaterals.

In summary, we have identified and characterized CHH cDNAs from two peracarid crustaceans, an underrepresented group in terms of CHH sequence identity, and mapped the localization of the mRNA and peptide to cells in the protocerebrum, reminiscent of staining patterns shown in terrestrial isopods. We exploited the tractable behavioral rhythmicity of these animals to test the hypothesis that CHH mRNA would be rhythmically expressed. Our data suggest CHH mRNA is constitutively expressed in these animals.

References

Alheit, J., Naylor, E., 1976. Behavioral basis of intertidal zonation in *Eurydice pulchra* Leach. J. Exp. Mar. Biol. Ecol. 23, 135-144.

Azzouna, A., Philippe, M., Jarry, T., Greve, P., Martin, G., 2003. Localization of crustacean hyperglycemic and vitellogenesis-inhibiting hormones in separate cell types in the protocerebrum of the woodlouse *Armadillidium vulgare* (Crustacea, Isopoda). Gen Comp Endocrinol 131, 134-142.

Beckwith, E.J., Lelito, K.R., Hsu, Y.W., Medina, B.M., Shafer, O., Ceriani, M.F., de la Iglesia, H.O., 2011. Functional conservation of clock output signaling between flies and intertidal crabs. J. Biol. Rhythms 26, 518-529.

Bregazzi, P.K., Naylor, E., 1972. Locomotor activity rhythm of *Talitrus saltator* (Montagu) (Crustacean, Amphipoda). J. Exp. Biol. 57, 375-391.

Castanon-Cervantes, O., Battelle, B., Fanjul-Moles, M.L., 1999. Rhythmic changes in the serotonin content of the brain and eyestalk of crayfish during development. J. Exp. Biol. 202 (Pt 20), 2823-2830.

Chang, E.S., Chang, S.A., Beltz, B.S., Kravitz, E.A., 1999. Crustacean hyperglycemic hormone in the lobster nervous system: localization and release from cells in the subesophageal ganglion and thoracic second roots. J. Comp. Neurol. 414, 50-56.

Chen, S.H., Lin, C.Y., Kuo, C.M., 2004. Cloning of two crustacean hyperglycemic hormone isoforms in freshwater giant prawn (*Macrobrachium rosenbergii*): evidence of alternative splicing. Mar. Biotechnol. 6, 83-94.

Chung, JS., Webster, SG., 2004. Expression and release patterns of neuropeptides during embryonic development and hatching of the green shore crab, *Carcinus maenas*, Development. 131(19), 4751-4761

Chung, J.S., Zmora, N., 2008. Functional studies of crustacean hyperglycemic hormones (CHHs) of the blue crab, *Callinectes sapidus* - the expression and release of CHH in eyestalk and pericardial organ in response to environmental stress. FEBS J. 275, 693-704.

Davey, M.L., Hall, M.R., Willis, R.H., Oliver, R.W.A., Thurn, M.J., Wilson, K.J., 2000. Five crustacean hyperglycemic family hormones of *Penaeus monodon*: complementary DNA sequence and identification in single sinus glands by electrospray ionization-fourier transform mass spectrometry. Mar. Biotechnol. 2, 80-91.

Dircksen, H., Bocking, D., Heyn, U., Mandel, C., Chung, J.S., Baggerman, G., Verhaert, P., Daufeldt, S., Plosch, T., Jaros, P.P., Waelkens, E., Keller, R., Webster, S.G., 2001. Crustacean hyperglycaemic hormone (CHH)-like peptides and CHH-precursor-related peptides from pericardial organ neurosecretory cells in the shore crab, *Carcinus maenas*, are putatively spliced and modified products of multiple genes. Biochem. J. 356, 159-170.

Escamilla-Chimal, E.G., Hiriart, M., Sanchez-Soto, M.C., Fanjul-Moles, M.L., 2002. Serotonin modulation of CHH secretion by isolated cells of the crayfish retina and optic lobe. Gen. Comp. Endocrinol. 125, 283-290.

Escamilla-Chimal, E.G., Van Herp, F., Fanjul-Moles, M.L., 2001. Daily variations in crustacean hyperglycaemic hormone and serotonin immunoreactivity during the development of crayfish. J. Exp. Biol. 204, 1073-1081.

Escamilla-Chimal, E.G., Velazquez-Amado, R.M., Fiordelisio, T., Fanjul-Moles, M.L., 2010. Putative pacemakers of crayfish show clock proteins interlocked with circadian oscillations. J. Exp. Biol. 213, 3723-3733.

Fanjul-Moles, M.L., Escamilla-Chimal, E.G., Gloria-Osorio, A., Hernandez-Herrera, G., 2004. The Crayfish *Procambarus clarkii* CRY shows daily and circadian variation. J. Exp. Biol. 207, 1453-1460.

Gorgels-Kallen, J.L., Voorter, C.E.M., 1985. The secretory dynamics of the CHH-producing cell group in the eyestalk of the crayfish, *Astacus leptodactylus*, in the course of the day-night cycle. Cell Tissue Res. 241, 361-366.

Greve, P., Sorokine, O., Berges, T., Lacombe, C., Van Dorsselaer, A., Martin, G., 1999. Isolation and amino acid sequence of a peptide with vitellogenesis inhibiting activity from the terrestrial isopod *Armadillidium vulgare* (Crustacea). Gen. Comp. Endocrinol. 115, 406-414.

Gu, P.L., Yu, K.L., Chan, S.M., 2000. Molecular characterization of an additional shrimp hyperglycemic hormone: cDNA cloning, gene organization, expression and biological assay of recombinant proteins. FEBS Lett. 472, 122-128.

Hall, T.A., 1999. Bioedit: A User Friendly biological sequence alignment editor and analysis program for Windows 95/98/NT, Nucleic Acid Symposium, pp. 95-98.

Harthoorn, L.F., Oudejans, R.C., Diederen, J.H., Van de Wijngaart, D.J., Van der Horst, D.J., 2001. Absence of coupling between release and biosynthesis of peptide hormones in insect neuroendocrine cells. Eur. J. Cell Biol. 80, 451-457.

Hastings, M.H., 1981a. The entraining effect of turbulence on the circatidal activity rhythm and its semi-lunar modulation in *Eurydice pulchra*. J. Mar. Biol. Assoc. UK 61, 151-160.

Hastings, M.H., 1981b. Semi-lunar variations of endogenous circa-tidal rhythms of activity and respiration in the isopod *Eurydice pulchra*. Mar. Ecol. Prog. Ser. 4, 85-90.

Kallen, J.L., Abrahamse, S.L., Vanherp, F., 1990. Circadian rhythmicity of the crustacean hyperglycemic hormone (CHH) in the hemolymph of the crayfish. Biol. Bull. 179, 351-357.

Kallen, J.L., Rigiani, N.R., Trompenaars, H.J.A.J., 1988. Aspects of entrainment of CHH cell activity and hemolymph glucose levels in crayfish. Biol. Bull. 175, 137-143.

Keller, R., Jaros, P.P., Kegel, G., 1985. Crustacean hyperglycemic neuropeptides. Am. Zool. 25, 207-221.

Lago-Leston, A., Ponce, E., Munoz, M.E., 2007. Cloning and expression of hyperglycemic (CHH) and molt-inhibiting (MIH) hormones mRNAs from the eyestalk of shrimps of *Litopenaeus vannamei* grown in different temperature and salinity conditions. Aquaculture 270, 343-357.

Manfrin, C., Tom, M., De Moro, G., Gerdol, M., Guarnaccia, C., Mosco, A., Pallavicini, A., Giulianini, P.G., 2013. Application of D-crustacean hyperglycemic hormone induces peptidases transcription and suppresses glycolysis-related transcripts in the hepatopancreas of the crayfish *Pontastacus leptodactylus* - results of a transcriptomic study. PLoS One 8(6): e65176. doi:10.1371/journal.pone.0065176

Marco, H.G., Brandt, W., Gade, G., 1998. Elucidation of the amino acid sequence of a crustacean hyperglycaemic hormone from the spiny lobster, *Jasus lalandii*. Biochem. Bioph. Res. Co 248, 578-583.

Martin , G., 1988. Immunocytochemistry and ultrastructure of crustacean endocrine cells. In: Thorndyke, M.C., Goldsworthy, G.J., (Eds.) Neurohormones in invertebrates Seminar Series vol 33. Cambridge University Press, pp. 79-96.

Martin, G., Jaros, P.P., Besse, G., Keller, R., 1984a. The hyperglycemic neuropeptide of the terrestrial isopod, *Porcellio dilatatus*. 2.

Immunocytochemical demonstration in neurosecretory structures of the nervous system. Gen. Comp. Endocrinol. 55, 217-226.

Martin, G., Keller, R., Kegel, G., Besse, G., Jaros, P.P., 1984b. The hyperglycemic neuropeptide of the terrestrial isopod, *Porcellio dilatatus*. 1. Isolation and characterization. Gen. Comp. Endocrinol. 55, 208-216.

Martin, G., Sorokine, O., Van Dorsselaer, A., 1993. Isolation and molecular characterization of a hyperglycemic neuropeptide from the sinus gland of the terrestrial isopod *Armadillidium vulgare* (Crustacea). Eur. J. Biochem. 211, 601-607.

Nelson-Mora, J., Prieto-Sagredo, J., Loredo-Ranjel, R., Fanjul-Moles, M.L., 2013. Putative pacemakers in the eyestalk and brain of the crayfish *Procambarus clarkii* show circadian oscillations in levels of mRNA for crustacean hyperglycemic hormone. PLoS One 8, e83937. doi:10.1371/journal.pone.0083937.

Nussbaum, T., Dircksen, H., 1995. Neuronal pathways of classical crustacean neurohomrones in the central nervous system of the woodlouse, *Oniscus asellus* (L) Philos Trans. R. Soc. Lond. B Biol. Sci. 347, 139-154.

O' Grady, J.F., 2013. Molecular biology of timekeeping in the beach amphipod *Talitrus saltator* (Montagu), PhD Thesis, Institute of Biological, Environmental and Rural Sciences. Aberystwyth University, UK.

O'Neill, J.S., Lee, K.D., Zhang, L., Feeney, K., Webster, S.G., Blades, M.J., Kyriacou, C.P., Hastings, M.H., Wilcockson, D.C., 2015. Metabolic molecular markers of the tidal clock in the marine crustacean *Eurydice pulchra*. Curr. Biol. 25, R326-327.

Ollivaux, C., Gallois, D., Amiche, M., Boscameric, M., Soyez, D., 2009. Molecular and cellular specificity of post-translational aminoacyl isomerization in the crustacean hyperglycaemic hormone family. FEBS J. 276, 4790-4802.

Qian, Y.Q., Dai, L., Yang, J.S., Yang, F., Chen, D.F., Fujiwara, Y., Tsuchida, S., Nagasawa, H., Yang, W.J., 2009. CHH family peptides from an 'eyeless' deep-sea hydrothermal vent shrimp, *Rimicaris kairei*: characterization and sequence analysis. Comp. Biochem. Phys. B 154, 37-47.

Sandeman, D., Sandeman, R., Derby, C., Schmidt, M., 1992. Morphology of the brain of crayfish, crabs, and spiny lobsters - a common nomenclature for homologous structures. Biol. Bull. 183, 304-326.

Santos, E.A., Keller, R., Rodriguez, E., Lopez, L., 2001. Effects of serotonin and fluoxetine on blood glucose regulation in two decapod species. Braz. J. Med. Biol. Res. 34, 75-80.

Serrano, L., Blanvillain, G., Soyez, D., Charmantier, G., Grousset, E., Aujoulat, F., Spanings-Pierrot, C., 2003. Putative involvement of crustacean hyperglycemic hormone isoforms in the neuroendocrine mediation of osmoregulation in the crayfish *Astacus leptodactylus*. J. Exp. Biol. 206, 979-988.

Sharp, J.H., Wilcockson, D.C., Webster, S.G., 2010. Identification and expression of mRNAs encoding bursicon in the plesiomorphic central nervous system of *Homarus gammarus*. Gen. Comp. Endocrinol. 169, 65-74.

Soyez, D., 2003. Recent data on the crustacean hyperglycemic hormone family, in: Fingerman, M., Nagabhushanam, R. (Eds.), Recent Advances in Marine Biotechnology. Sciences Publishers, Enfield, NH, USA, Plymouth, UK, pp. 279-301.

Soyez, D., Laverdure, A.M., Kallen, J., VanHerp, F., 1998. Demonstration of a cell-specific isomerization of invertebrate neuropeptides. Neuroscience 82, 935-942.

Soyez, D., Toullec, J.Y., Ollivaux, C., Geraud, G., 2000. L to D amino acid isomerization in a peptide hormone is a late post-translational event occurring in specialized neurosecretory cells. J. Biol. Chem. 275, 37870-37875.

Soyez, D., Van Herp, F., Rossier, J., Le Caer, J.P., Tensen, C.P., Lafont, R., 1994. Evidence for a conformational polymorphism of invertebrate neurohormones. D-amino acid residue in crustacean hyperglycemic peptides. J. Biol. Chem. 269, 18295-18298.

Stefanini, M., De Martino, C., Zamboni, L., 1967. Fixation of ejaculated spermatozoa for electron microscopy. Nature 216, 173-174.

Tamura, K., Stecher, G., Peterson, D., Filipski, A., Kumar, S., 2013. MEGA6: Molecular Evolutionary Genetics Analysis Version 6.0. Mol. Biol. Evol. 30, 2725-2729.

Tilden, A., McGann, L., Schwartz, J., Bowe, A., Salazar, C., 2001. Effect of melatonin on hemolymph glucose and lactate levels in the fiddler crab *Uca pugilator*. J. Exp. Zool. 290, 379-383.

Tilden, A.R., McCoole, M.D., Harmon, S.M., Baer, K.N., Christie, A.E., 2011. Genomic identification of a putative circadian system in the cladoceran crustacean *Daphnia pulex*. Comp Biochem Physiol Part D Genomics Proteomics 6, 282-309.

Webster, S.G., 2015. Endocrinology of metabolism and water balance: crustacean hyperglycemic hormone, in: Chang, E.S., Thiel, M. (Eds.), The Natural History of the Crustacea, vol 4. Oxford University Press, USA, pp. 37-67.

Webster, S.G., Dircksen, H., Chung, J.S., 2000. Endocrine cells in the gut of the shore crab *Carcinus maenas* immunoreactive to crustacean hyperglycaemic hormone and its precursor-related peptide. Cell Tissue Res. 300, 193-205.

Webster, S.G., Keller, R., Dircksen, H., 2012. The CHH-superfamily of multifunctional peptide hormones controlling crustacean metabolism, osmoregulation, moulting, and reproduction. Gen. Comp. Endocrinol. 175, 217-233.

Wilcockson, D.C., Chung, J.S., Webster, S.G., 2002. Is crustacean hyperglycaemic hormone precursor-related peptide a circulating neurohormone in crabs? Cell. Tissue Res. 307, 129-138.

Wilcockson, D.C., Zhang, L., Hastings, M.H., Kyriacou, C.P., Webster, S.G., 2011. A novel form of pigment-dispersing hormone in the central nervous system of the intertidal marine isopod, *Eurydice pulchra* (Leach). J. Comp. Neurol. 519, 562-575

Yasuda, A., Yasuda, Y., Fujita, T., Naya, Y., 1994. Characterization of crustacean hyperglycemic hormone from the crayfish (*Procambarus clarkii*) - multiplicity of molecular forms by stereoinversion and diverse functions. Gen. Comp. Endocrinol. 95, 387-398.

Zhang, L., Hastings, M.H., Green, E.W., Tauber, E., Sladek, M., Webster, S.G., Kyriacou, C.P., Wilcockson, D.C., 2013. Dissociation of circadian and circatidal timekeeping in the marine crustacean *Eurydice pulchra*. Curr. Biol. 23, 1863-1873.

Figure legends

Figure 1
A: CHH nucleotide and deduced amino acid sequences for *E. pulchra*. Nucleotide numbering begins at the 5' UTR (-64), ATG (bold text) at +1, and stop codon (black box, asterisk) at +363; polyadenylation signal is shown as an open box. Grey boxed sequence depicts putative signal peptide, and underlined sequence indicates deduced mature CHH amino acid sequence, including amidation signal immediately followed a dibasic cleavage site. B: CHH nucleotide and deduced amino acid sequence for *T. saltator*. Boxes, lines and symbols indicate features as described above for *E. pulchra* but with a stop codon positioned at +404.

Figure 2
Localization of CHH peptide and mRNA in the cerebral and optic ganglia.
A: Immunoreactivity to anti CHH IgG in the cerebral ganglion of *E. pulchra*. Eight perikarya were visualized from which a large axon tract (white arrowheads) emanates, heading laterally along the ventro-lateral margin of the optic ganglia to the sinus gland (B). The main tract bifurcates (red arrow) with less intensely stained fibers turning posteriorly leading through the deuterocerebrum (white arrows) and ending adjacent to the esophageal orifice in the tritocerebrum (*). Collaterals close to the cell bodies form dendritic fields anteriorly. B-C: Intense labelling in the sinus gland of *E. pulchra* and *T. saltator*, respectively. D: Immunoreactive perikarya in protocerebrum of *T. saltator*. Six perikarya were evident and as for *E. pulchra* a heavily labelled primary axon tract emerged from these cells and turned laterally (white arrow head) into the optic lobe. A bifurcation of the primary tract gave rise to fibers passing posteriorly through the deuterocerebrum (white arrows) and terminating in the tritocerebrum (*). Proximal collaterals form dendritic fields adjacent and slightly posterior the perikarya. E: Enlargement of CHH immunopositive perikarya seen in *T. saltator* showing two distinct cells types. Three large (35µM) and three small (23µm) were labelled. Fine arborizing dendrites, from proximal collaterals. Larger, apparently swollen endings are evident. F-G: CHH mRNA localization by *insitu* hybridization for *E. pulchra* and *T. saltator,* respectively. DIG incorporated antisense riboprobes specifically labelled cells in the anterior protocerebrum, exactly as described by immunlocalization. Sense probes resulted in no specific staining (not shown).

Figure 3
Activity rhythms of *E. pulchra* and *T. saltator*.
Representative actograms from A: individual *E. pulchra* and B: *T. saltator* held in DD after natural entrainment and LD12:12 entrainment respectively. Subjective day and night are shown above plot B by grey and black bars. C: Chi-squared periodogram analysis of *E. pulchra* and *T. saltator* locomotor activity (as plotted in A-B) revealed a tau of 12.3 and 23.8h respectively (red line denotes p<0.01-amplitude exceeding this line is taken as significant). E-F: Mean activity (+SEM) of animals recorded in activity monitors. Infrared beam breaks were collected at 10- second intervals and pooled into 6-minute bins. Red arrows on plot E show

time of expected high water on the home beach whilst subjective day and night are shown by grey and black bars respectively.

Figure 4
Quantitative RT-PCR gene expression profiling of CHH mRNA in heads of behaviorally rhythmic *E. pulchra* and *T. saltator* sampled under free-running (DD) light conditions. A: *E. pulchra*; B: *T saltator*. Neither species exhibited significant changes in *Chh* gene expression over a 24h time-course (ANOVA, $F_{(7, 24)}$=1.19, P=0.35 and $F_{(8, 45)}$=0.72, P=0.67). *Chh* values were normalised to the reference genes *erpl32* and *talAK* and expressed as copy number per copy of the reference gene. Grey and black bars indicate the time subjective daytime and nighttime, respectively. For *E. pulchra*, the abscissa tick-marks show the solar time and tidal intervals (HW=high water, LW= low water) whilst for *T. saltator* they show circadian time, where 24/0h is dawn (lights on). Arrowheads on plot A depict time of expected high water on the home beach.

Supplementary Figure 1
Molecular Phylogenetic analysis of known CHHs. The evolutionary history was inferred by using the Maximum Likelihood method based on the Poisson correction model with 1000 bootstrap replications. The tree was constructed using sequences derived from eyestalk or brain tissues and mature peptide sequences. Branches indicate bootstrap support values. Accession numbers for peptide sequences:
*Locusta migratoria ITP,* AAD20820*, Daphnia magna* ITP, ABO43963; *Armadillidium vulgare*, P30814; *Eurydice pulchra*, JF927891; *Astacus astacus,* P83800; *Bythograea thermydron*, AAK28329; *Callinectes sapidus*, AAS45136; *Cancer pagurus*, P81032; *Cancer productus* CHHI, ABQ41269; *Carcinus maenas*, P14944; *Cherax destructor CHHA*, P83485; *Chionoecetes bairdi*, ACG50068; *Galathaea strigosa*, ABS01332; *Discoplax celeste*, JF894384; *Gecarcinus lateralis*, ABF48652; *Gecarcoidea natalis*, ABL09570; *Grapsus tenuicrustatus*, JN048801; *Homarus americanus* CHHA, P19806; *Homarus americanus* CHHB, Q25154; *Homarus gammarus* CHHA, ABA42179; *Jasus lalandii*, P56687; *Libinia emarginata*, AAD32706; *Litopenaeus schmitti*, P59685; *Litopenaeus vannamei*, CAA68067; *Macrobrachium rosenbergii*, AAL40915; *Marsupenaeus japonicus* CHH1, O15980; *Metapenaeus ensis* CHHA, AAD45233; *Nephrops norvegicus* CHHA, AY285782; *Orconectes limosus*, Q25589; *Pachygrapsus marmoratus*, AAO27804; *Pagarus bernhardus*, ABE02191; *Peneaus monodon* CHH1, O97383; *Pontastacus leptodactylus,* AAX09331; *Portunus trituberculatus*, EU395808; *Potamon ibericum*, ABA70560; *Procambarus clarkia*, AB027291; Ptychognathus pusillus, JN048802; *Procambarus bouvieri*, Q10987; *Rimicaris kairei*, FJ447499; *Scylla olivacea*, AY372181; *Talitrus saltator*, KP898735.

A

gaaa

actttgacaacagctcttgtgtctaatagtatttccagaacacaaccaaacaaaaccgaa

+1
atgttttcctcaaagctttctgcatcggtagtggccgtgtgggtggtggttctgctgtgt
　M　F　S　S　K　L　S　A　S　V　V　A　V　W　V　V　V　L　L　C

atagcagaaacgggcgaaggacgaaatatggaaccttctacactggacagactaaataac
　I　A　E　T　G　E　G　R　N　M　E　P　S　T　L　D　R　L　N　N

gcaaaggccaaacgacaagtgtttgacgcaagctgtaaaggaatctacgacagggaactc
　A　K　A　K　R　Q　V　F　D　A　S　C　K　G　I　Y　D　R　E　L

ttcagccaactggaacgcgtttgcgaggactgttacaacctctacagaaagcctgtcgtc
　F　S　Q　L　E　R　V　C　E　D　C　Y　N　L　Y　R　K　P　V　V

gctactgaatgcaggagagaatgctacacaactgaggtcttcgaaagttgtctccgtgac
　A　T　E　C　R　R　E　C　Y　T　T　E　V　F　E　S　C　L　R　D

cttatgatgcatgaccttattaacgaatacaaagaaaaggcgtacatggttgctggcaag
　L　M　M　H　D　L　I　N　E　Y　K　E　K　A　Y　M　V　A　G　K

+363
aaataaaaacaagcattacaccactccagagtcaatggcagtagtaccgattgttttta
　K　*

aaatatatatgtgacagtttattaaggttgctagagatccaagctctcatgaatattaat

taagaattagttttttgtatcagaatgaagtgt[aataaa]cattgcatcgtagaaaaaaaa

aaaaaaaaaaa

B

gaattttcacgcttccctttaccacgtttttactgacaacgtgaaatcgaaatacgaaatt

ctagctctattctacttttataaggggaacaagttccgtcagacgacagcccgagctacc

tcaggtcctcgaccgcctcctgaaccagcgccatc**atg**tcaccagttgccgtcaccgctg
　　　　　　　　　　　　　　　　　　　M　S　P　V　A　V　T　A

cagtcgtcgttgccttgatcgtcatgagctccagccactcctcagcgtcccctgagatgc
　A　V　V　A　L　I　V　M　S　S　S　H　S　S　A　S　P　E　M

tcgagaagtcacttcagcggtcgtcgcgcctgctgacgtccccatccacgggccgctacc
　L　E　K　S　L　Q　R　S　S　R　L　L　T　S　P　S　T　G　R　Y

ccttctcccgtctgctggccaacagggggtccctgctggcgggagacgccggccgctcct
　P　F　S　R　L　L　A　N　R　G　S　L　L　A　G　D　A　G　R　S

cccttctctccactgacctcggaaggcccaagcgggccctctttgatgactcctgcaagg
　S　L　L　S　T　D　L　G　R　P　K　R　A　L　F　D　D　S　C　K

gcgtctacgacagagagctcttcgctaaactggaccgcgtctgcgaggactgctacaacc
　G　V　Y　D　R　E　L　F　A　K　L　D　R　V　C　E　D　C　Y　N

tctacaggaagcccagcgtctcttacgagtgcaggcgagactgctacagcaacgcgatgt
　L　Y　R　K　P　S　V　S　Y　E　C　R　R　D　C　Y　S　N　A　M

tcgagagctgcctctacgacctcatgctgcacgagatggtcgacaagtacgctgaaatgg
　F　E　S　C　L　Y　D　L　M　L　H　E　M　V　D　K　Y　A　E　M

+404
tccagattgtggggcaagaaataaccagcaatgactactctcataacctggtatttta
　V　Q　I　V　G　K　K　*

cgctacatcgaagccgaattacgacaataactcccctcatgaaacgcttccatcgctgct

agtatttattgaagatctcgttaagcaacaacacaatgccctggccattaagaaactatc

ttctcgagtccacaaatcaagacacttcgtctgtgtgccgctgggccttgtacgaactac

caggacaagcttctcgtctctggccaaacttcgtcagactgataaaaagtaaaataactc

tcacgaatgatggaaatgggctgacgcttacacacccgtcatcaactgtggctgatcagg

gaaccgccgggcaacaccgtttcattcgacggtaggcagatgcatattgtaataacagag

ttctgtagactcaagttacaagaaaatgaacccctagcagccgcaattcatgtatcaact

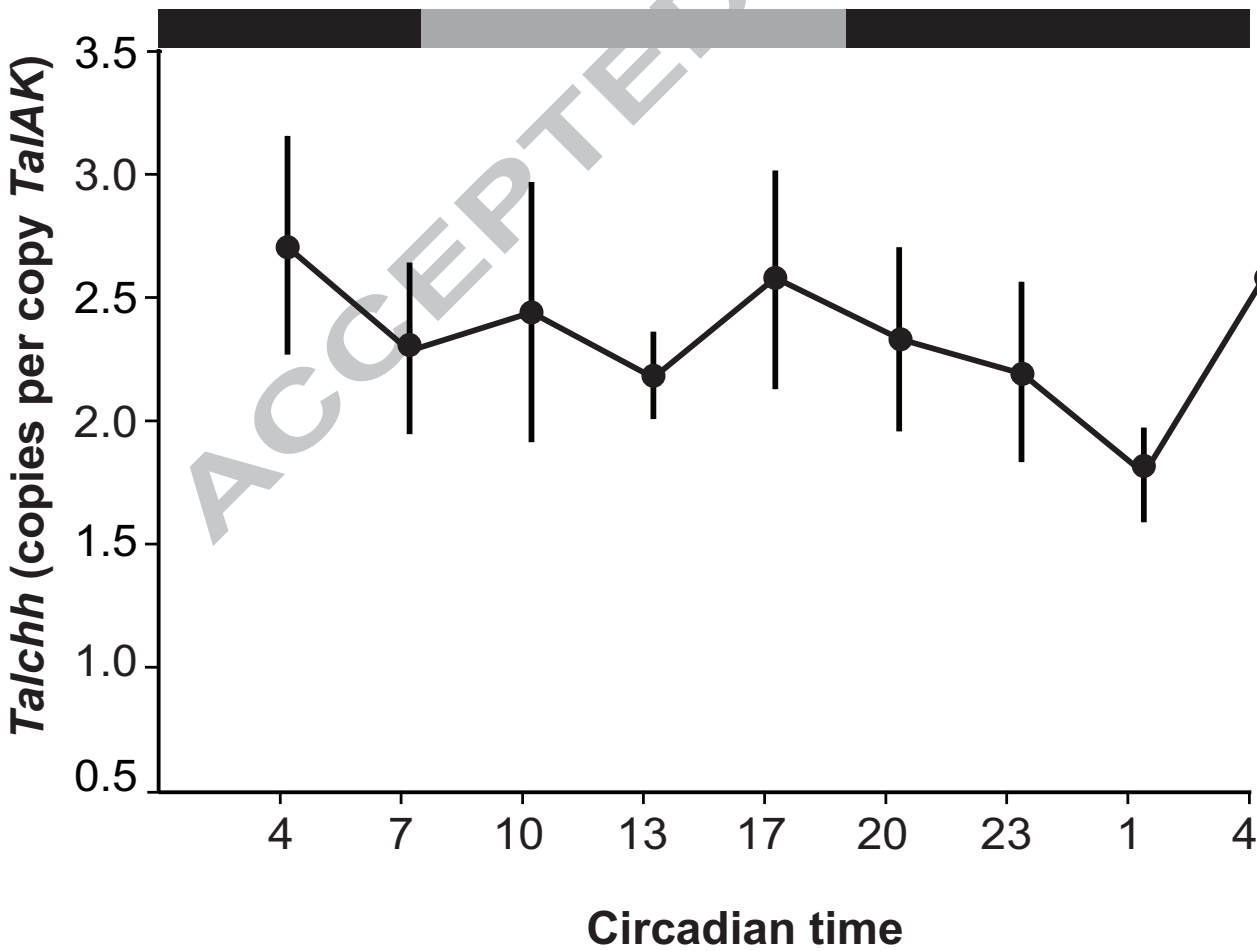atggttt[aataaaa]tttcaagcatctttaaaaaaaaaaaaaaaaaaaaaaaaaaa
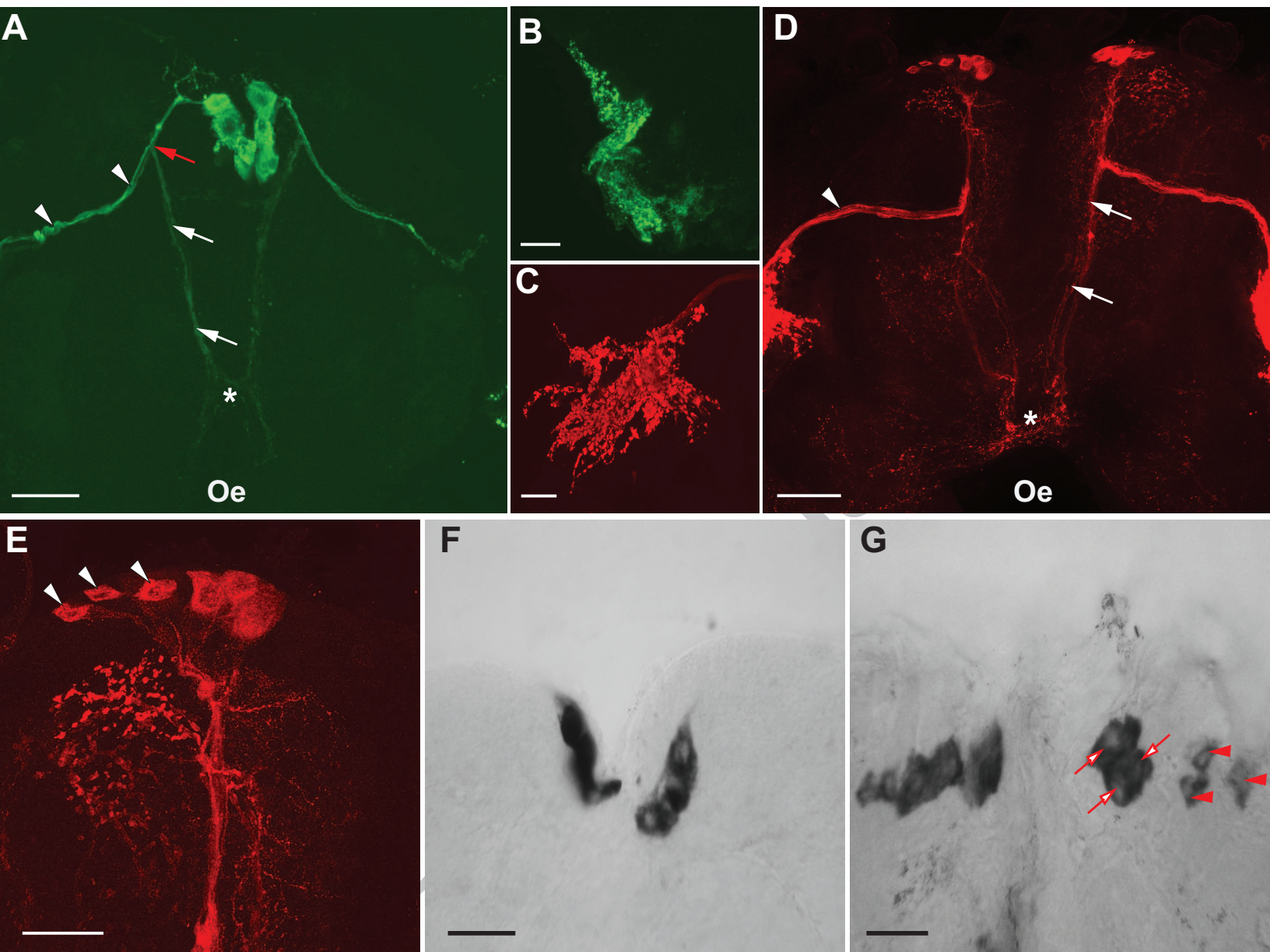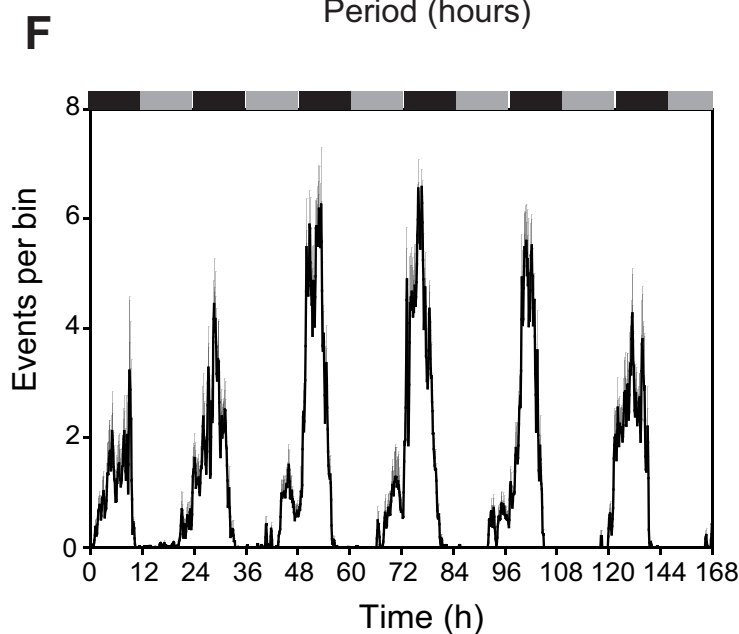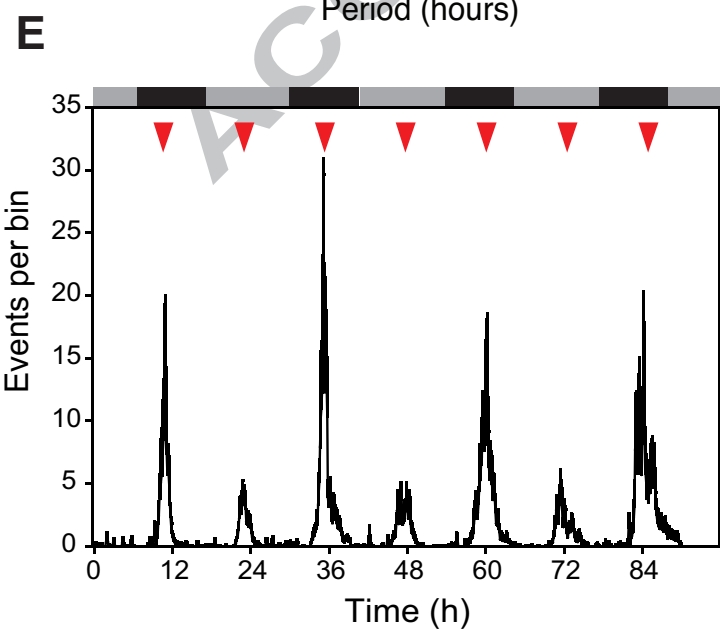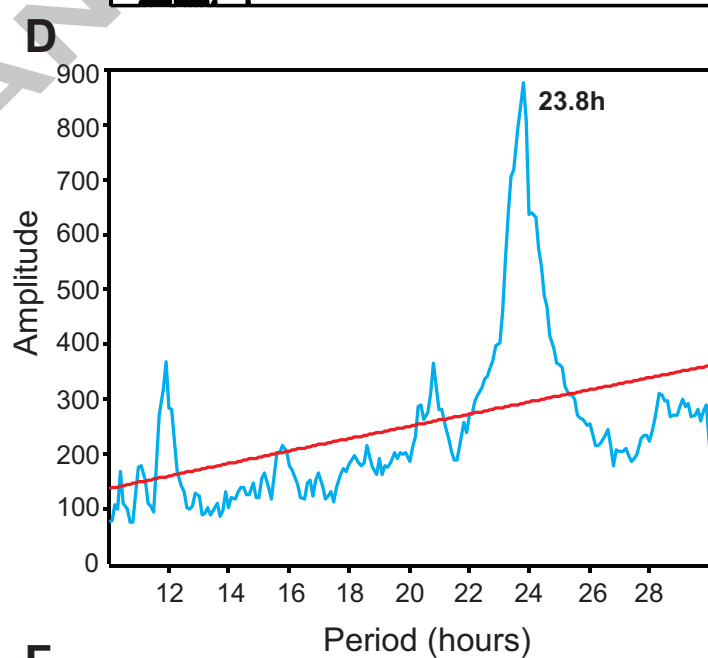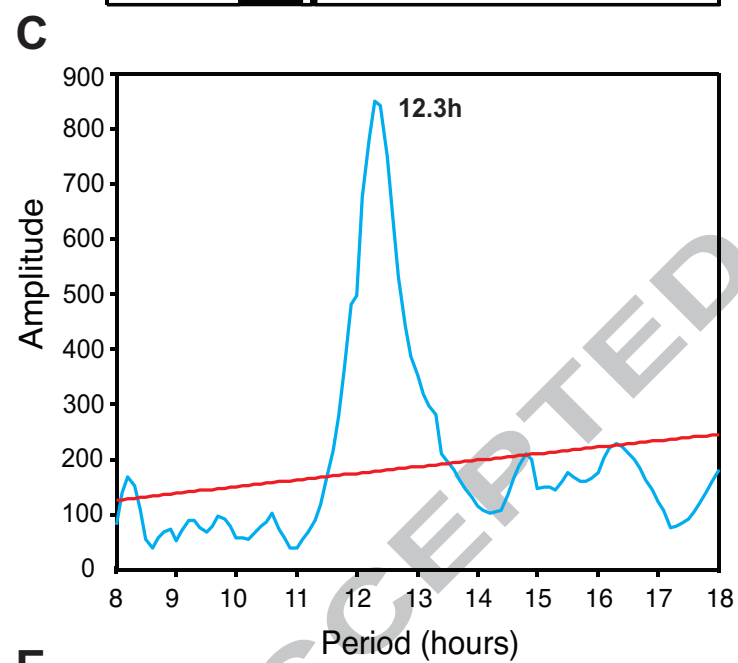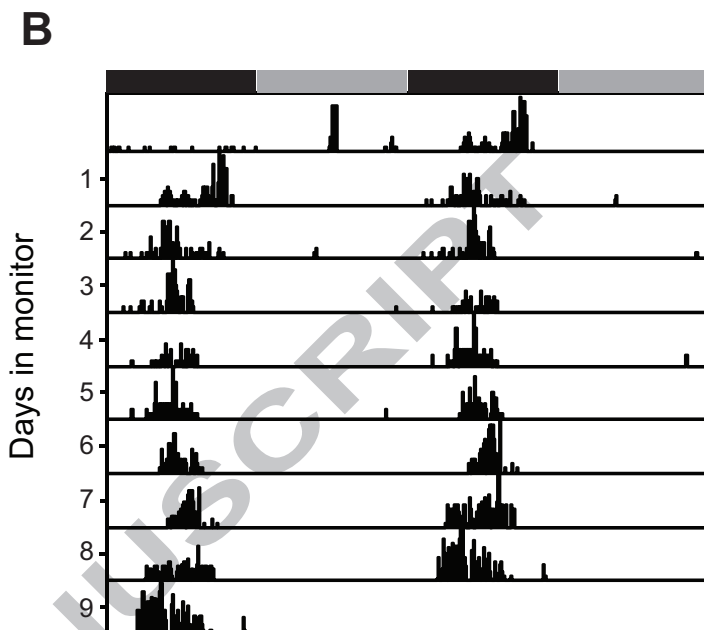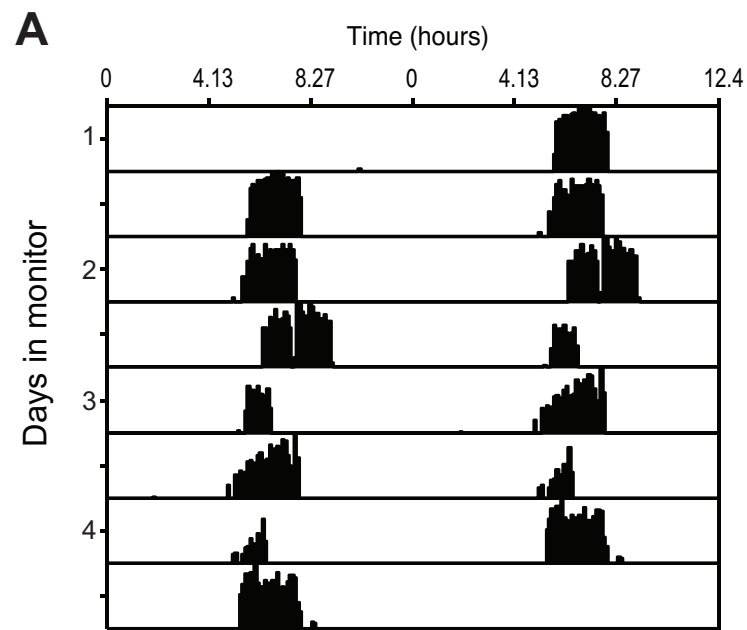
A
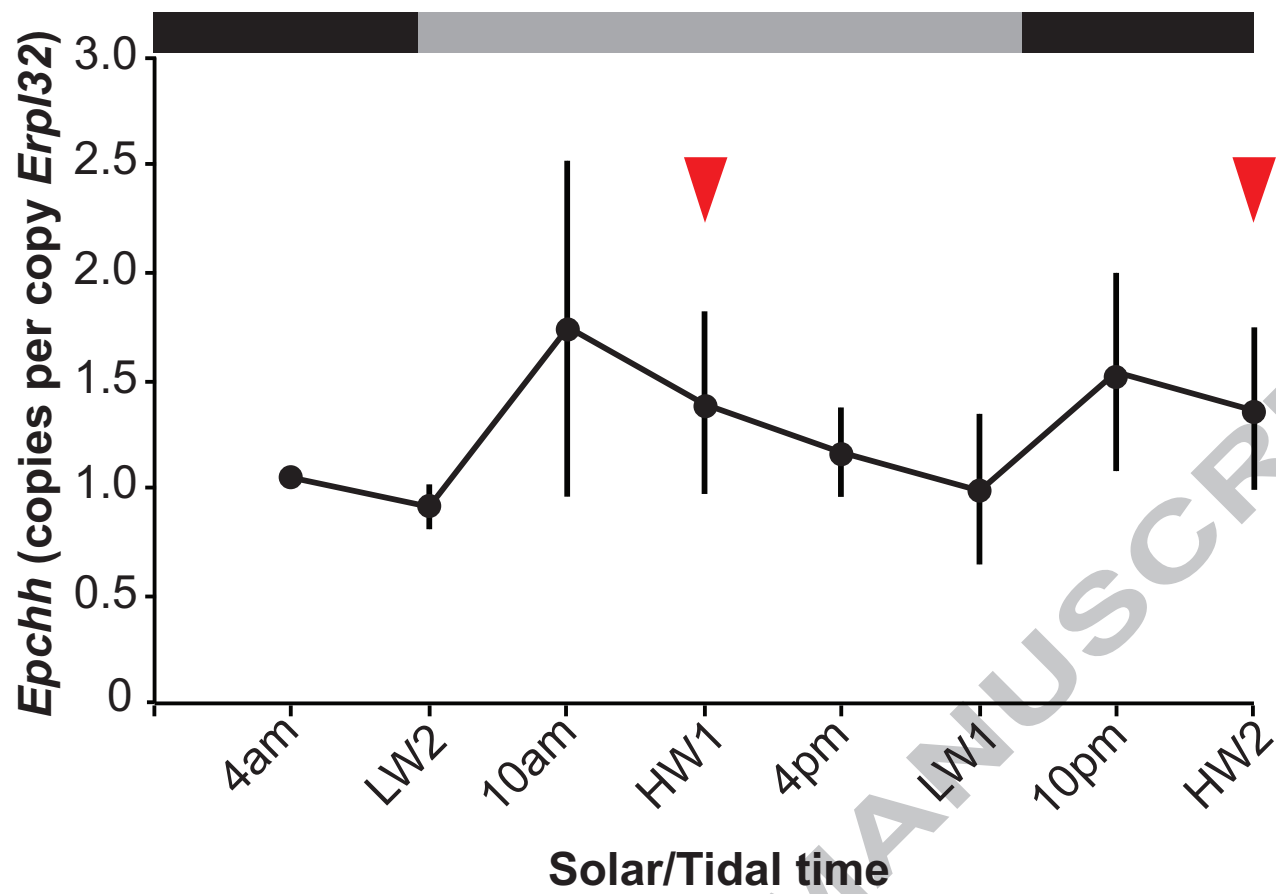
B

Highlights

- A hyperglycemic hormone cDNA was characterized in two peracarid crustaceans
- CHH was localized in the cerebral ganglia and showed striking similarities between species
- Each species exhibited robust, endogenous circatidal or circadian activity rhythms
- Temporal expression of CHH mRNA was neither circadian nor circatidal